

Flux Pinning Concepts for On-orbit Capture and Orientation of an MSR Orbiting Sample Container

Paulo Younse, Laura Jones-Wilson,
William Jones-Wilson, Ian McKinley,
Edward Gonzales, Boyan Kartolov,
Dima Kogan, Chi Yeung Chiu
Jet Propulsion Laboratory
California Institute of Technology
Pasadena, CA 91109 USA
paulo.j.younse@jpl.nasa.gov

Eric Olds, Violet Malyan
Sierra Lobo, Inc.
Pasadena, CA 91107 USA
eolds@sierralobo.com

Abstract—Concepts for on-orbit capture and orientation of a Mars orbiting sample container (OS) using flux pinning were developed as candidate technologies for potential Mars Sample Return (MSR). The systems consist of a set of type-II superconductors field cooled below their critical temperature using a cryocooler, and operate on an orbiting sample container with a series of permanent magnets spaced around the exterior, along with an integrated layer of shielding to preserve the magnetic properties of the returned samples. Benefits of the approaches include passive, non-contact capture and orientation, as well as a reduction in the number of actuators relative to various mechanical methods. System prototypes were developed, characterized, and tested in a microgravity environment to demonstrate feasibility. Flux pinning models were developed that accounts for magnet

geometry, superconductor geometry, superconductor training geometry, superconductor temperature, superconductor material properties, and magnetic field shape, and output forces and torques the superconductors imparts on the OS via the magnets. Magnetic models of the OS were developed to evaluate magnetic shield effectiveness and demonstrate successful shielding of the sample. A vision system using AprilTag fiducials was used on a free-floating OS in a microgravity environment to estimate relative OS position and orientation while in motion. Integrated Capture, Containment, and Return System (CCRS) Capture and Orient Module (COM) payload concepts for an Earth Return Orbiter (ERO) using flux pinning were proposed and assessed based on relevant system evaluation criteria, such as mass, actuator count, and power consumption.

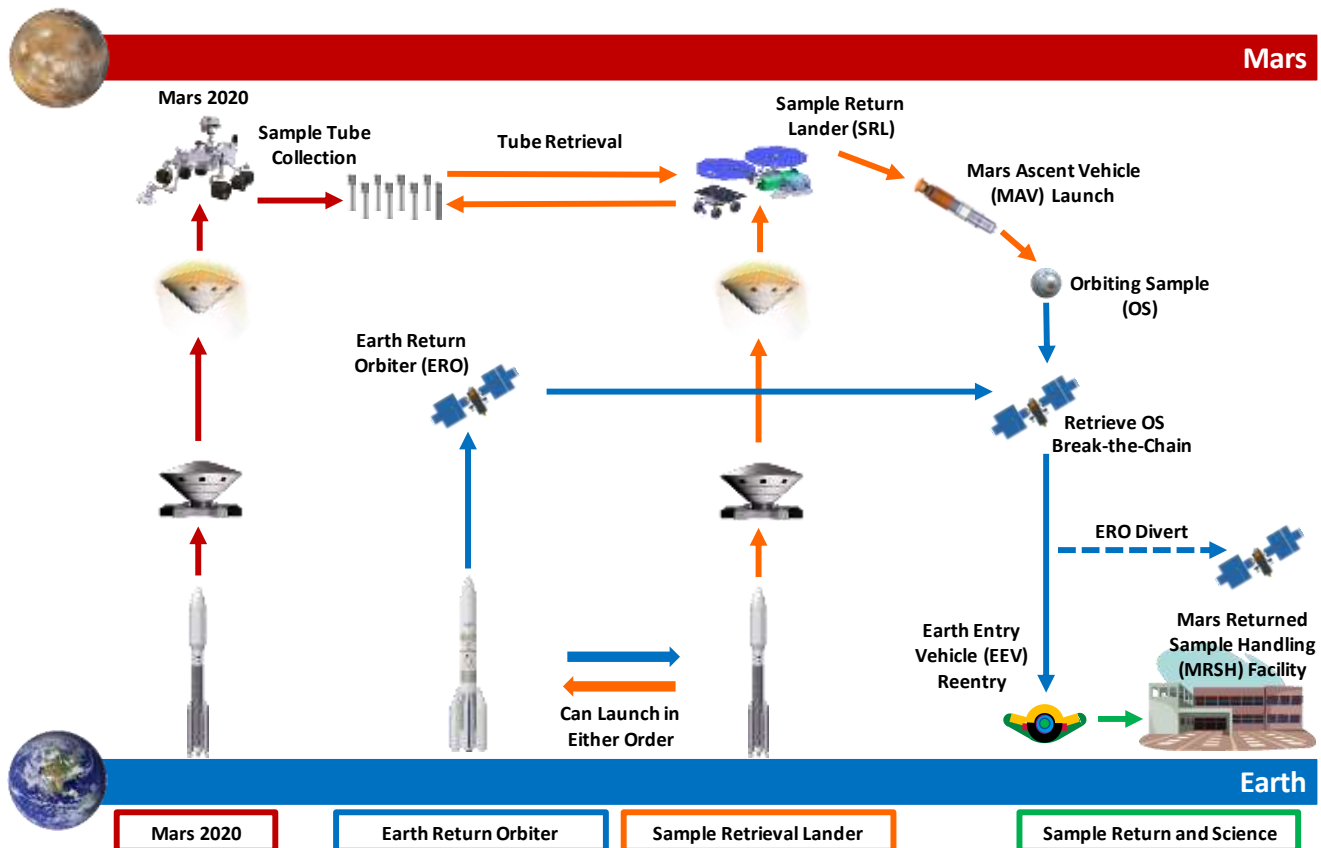


Figure 1: Notional MSR architecture. Note that all elements beyond Mars 2020 are conceptual.

TABLE OF CONTENTS

1. INTRODUCTION	2
2. BACKGROUND	3
3. PROBLEM DEFINITION.....	4
4. SYSTEM DESIGN.....	5
5. ANALYSIS	12
6. EXPERIMENTAL TESTING	14
5. DISCUSSION.....	17
6. CONCLUSION.....	17
ACKNOWLEDGEMENTS.....	18
REFERENCES.....	18
BIOGRAPHY	20

1. INTRODUCTION

Making significant progress towards Mars Sample Return (MSR) was highlighted as a high-priority goal for the decade 2013-2022 by the 2011 Planetary Decadal Survey [1]. A notional MSR campaign architecture, as shown in Fig. 1, consists of four elements: the Mars 2020 rover to acquire a set of samples and place them in a series of depots on the ground, a Sample Return Lander (SRL) with a fetch rover to recover the samples and launch them into Mars orbit in an Orbiting Sample (OS) container aboard a Mars Ascent Vehicle (MAV), an Earth Return Orbiter (ERO) to retrieve the OS from Mars orbit (see Fig. 2) and return it to Earth within an Earth Entry Vehicle (EEV), and a Sample Return and Science element consisting of a Mars Returned Sample Handling Facility to recover, receive, and curate the return samples.

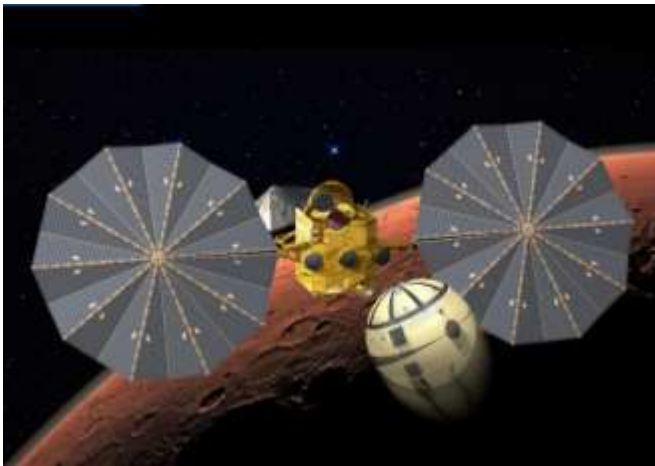


Figure 2. Artist's concept of Orbiting Sample (OS) capture in Mars orbit (Credit: D. Hinkle).

Capture, Containment, and Return System

In order for the ERO to retrieve the OS, a Capture, Containment, and Return System (CCRS) payload could be mounted onto the spacecraft bus (see Fig. 3). The primary functions of the CCRS would be to:

- Capture the OS in low Mars orbit to allow for retrieval back to Earth
- Contain the OS to prevent exposing unsterilized Mars material in or on the surface of the OS to the Earth's biosphere to meet Backward Planetary Protection concerns
- Return the OS to Earth within the EEV while ensuring the scientific integrity of the samples in all credible environments through landing on Earth

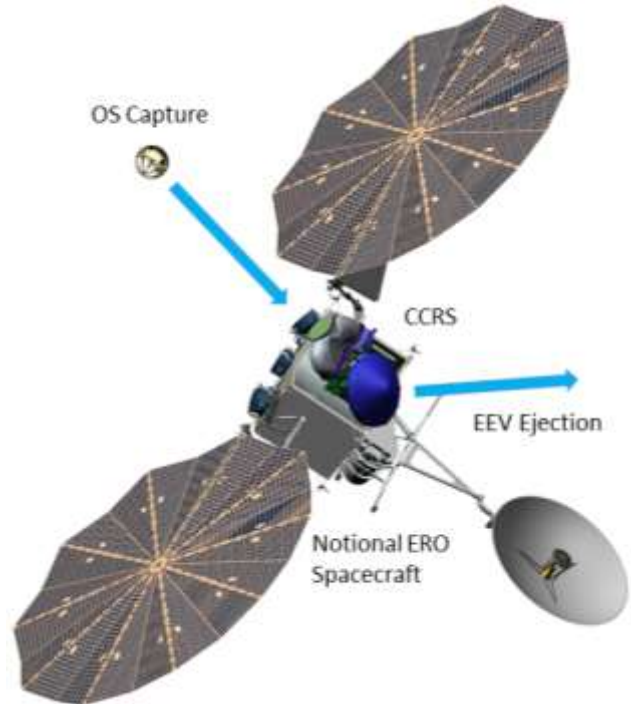


Figure 3. Notional Earth Return Orbiter with CCRS.

In addition to the capture, containment, and return functions, two additional functions were specified for the CCRS: OS reorientation and CCRS mass jettison at Mars orbit. The OS reorientation function allows the CCRS to orient the OS in an upright orientation relative to the EEV to minimize damaging impact loads on the sample tube hermetic seals during landing, improving probability of the EEV to preserve the returned sample science. The CCRS mass jettison function allows the CCRS to minimize mass required for the ERO to return to Earth, allowing for a faster Earth return. These functions were allocated to three modules within the CCRS: the Capture and Orient Module (COM), the Containment Module (CM), and the Earth Return Module (ERM). A notional CCRS concept with the three modules and their functions is shown in Fig. 4.

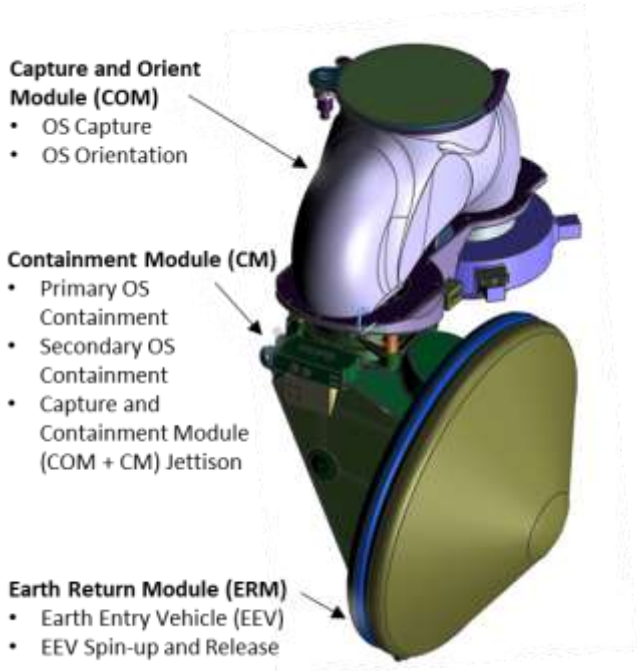


Figure 4. Notional CCRS with COM, CM, and ERM.

Application of Flux Pinning Technology to the Capture and Orientation Module

The research described in this paper investigates several Capture and Orientation Module architectures that use flux pinning technology to accomplish its functions. Benefits of flux pinning include the absence of actuated mechanisms, deterministic operations, non-contact manipulation, independence of friction, and compatibility with various OS shapes. A flux pinning system would require magnets on the OS, as well as shielding around the sample tubes to limit the exposure of the samples to magnetic fields that could affect their science value. Flux pinning would require a set of superconductors, a cryocooler, and radiator, as well as a field cooling operation prior to OS capture and orientation. Additional electromagnets would be required if the control rotation of the OS is desired for inspection. Verification and validation could be performed through a microgravity test flight on the ISS.

2. BACKGROUND

Previous research has been performed on OS capture and orientation technologies for Mars Sample Return, including methods involving flux pinning.

Sample Capture and Orientation Research

Concepts for an OS capture, containment, and return system have been developed and prototyped at NASA’s Jet Propulsion Laboratory (JPL) [2], [3], [4], [5]. Recent architectures for CCRS systems include the Rendezvous and OS Capture System (ROCS) Mars Capture and ReOrientation for Earth return (MACARONE) architecture (see Fig. 5) [2], [6], as well as an Inline architecture (see Fig. 6).

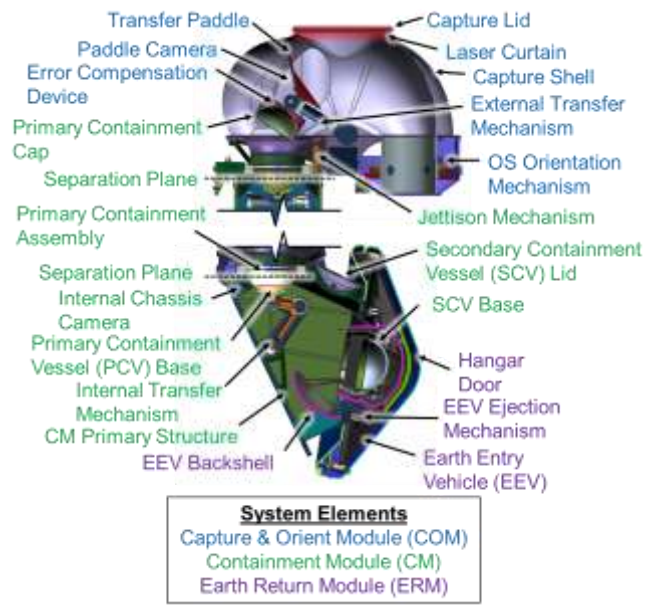


Figure 5. MACARONE architecture [6].

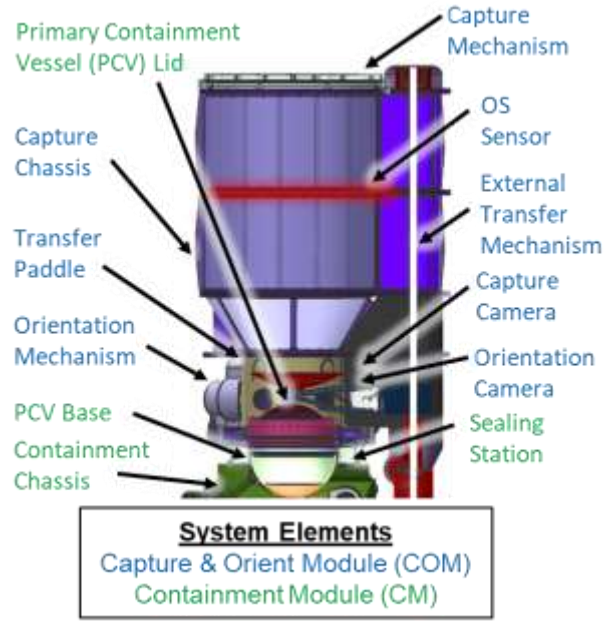


Figure 6. Inline architecture.

Flux Pinning Effect

Magnetic flux pinning is a phenomenon in superconducting physics where a type-II superconductor interacts with a magnetic field to create a passively stable non-contacting equilibrium between them [7], [8]. The superconductor experiences a material phase transition below its critical temperature, which results in zero internal resistance [9], [8]. If a magnet is placed near the superconductor during this transition, a process known as field cooling, the magnetic field will generate supercurrent vortices in the superconducting material. These supercurrent vortices react to changes in magnetic flux that generate forces and torques that act to restore the system to the equilibrium set at the magnet’s relative position to the superconductor during the

field-cooling process. This effect allows for a magnet to levitate with respect to the superconductor in a 1-g environment (see Fig. 7), and has general applications to frictionless bearings [10] and maglev trains [11].



Figure 7. A magnet (top) flux-pinned to a type-II superconductor disk (bottom).

When applied to close-proximity spacecraft dynamics, where one spacecraft is populated with an array of magnets and the other is outfitted with a set of superconductors field-cooled to set a desired equilibrium, the resulting flux-pinned interface (FPI) can result in a capture and re-orientation behavior of one spacecraft relative to the other without any active dynamics control [12]. Cornell University was the first to propose applying these physics to close-proximity spacecraft [13], and their research has examined a variety of applications including docking [14], formation flying [12], and non-contacting grappling [15]. JPL has been collaborating with Cornell to study this technology for a potential sample capture mission [16]. Drawing on more mature cooling designs for the superconductors [17], test data from a series of microgravity flight campaigns [16], [18], [19], and more mature models for flux pinning effects [18], this work ties together the overall design implications of a flux-pinned interface in a sample capture concept (see Fig. 8).

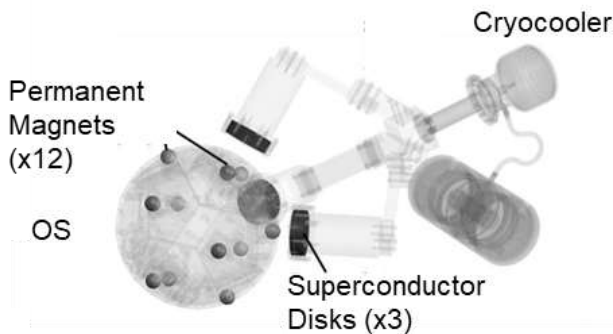


Figure 8. Concept utilizing flux pinning as a means for performing OS capture [16].

3. PROBLEM DEFINITION

The primary functions of the Capture and Orient Module are to capture the OS in low Mars orbit and orient the OS upright relative to the EEV. Additionally, there is desire to enclose the OS within the Capture and Orient Module prior to OS contact with the any CCRS hardware during OS capture to contain all Mars material that may be liberated from the OS from physical contact. This contained material can then be either jettison away or sterilized prior to Earth return. Doing so could help prevent unsterilized Mars particles from migrating from the CCRS to the ERO spacecraft, which could contaminate the spacecraft and increase the risk of exposing the Earth’s biosphere to unsterilized Mars particles in a case where the ERO spacecraft is unable to divert from Earth after EEV release.

The OS is assumed to be a maximum of 28 cm in diameter and 12 kg in mass. Fig. 9 shows a notional design of the OS in an upright orientation, defined by the OS reference axis, which ensures that the sealed sample tubes face upright during EEV landing. Visual features, such as fiducials, may be implemented on the OS to assist in OS pose estimation, orientation verification, and tracking of the OS during testing and operations. In the research described in this paper, AprilTags [20] were implemented into the conceptual OS design and prototype testing for assessing vision-based OS tracking and pose estimation.

To contain the OS, a set of primary and secondary containers could be used to provide redundant containment (see Fig. 10) [21]. Since the Capture and Orient Module is responsible for its initial manipulation, it’s assumed that the Module should assist in assembling the OS in the Primary Containment Vessel in preparation for sealing within the Containment Module. Because of this, it’s assumed that the capture and orientation elements should accommodate the geometry of the Primary Containment Vessel lid, which could be up an estimated 30 cm in diameter.

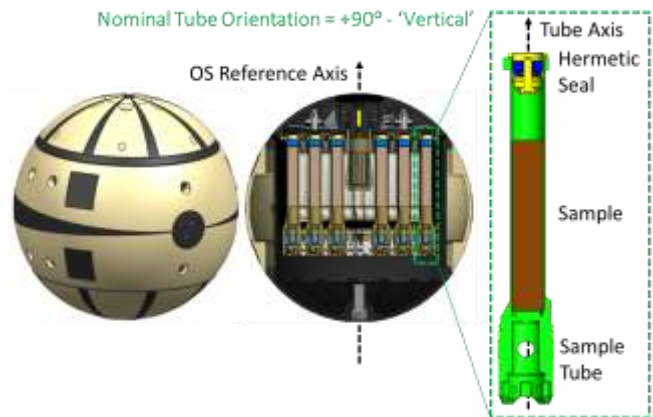


Figure 9. Notional OS with sample tubes [2], [22].

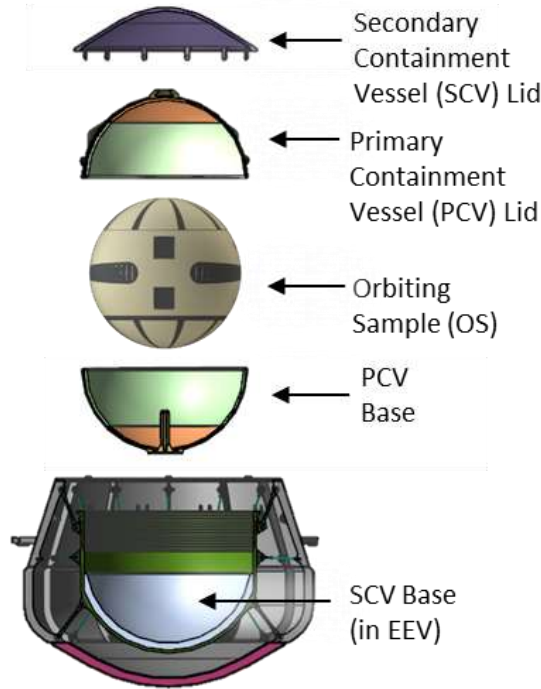


Figure 10. Potential OS containment strategy [2].

Evaluation Criteria

A set of system attributes were used to evaluate the Capture and Orient Module flux pinning concepts. Definitions of the attributes and rationale for their selection is shown in Tab. 1. For the mass attributes, Maximum Expected Value (MEV) was calculated by estimating a Current Best Estimate (CBE) basic value for mass, and then adding a Mass Growth Allowance (MGA) based on guidelines defined in ANSI/AIAA S-120A-2015. For the peak power attribute, Peak Power was calculated by estimating a Basic Power, and then adding a Power Growth Allowance (PGA) based on guidelines defined in AIAA S-122-2007.

Table 1: List of criteria used to evaluate the flux pinning Capture and Orient Module alternatives.

Criteria		Definition, Units	Rationale
Category	Attribute		
System Mass	COM Mass	Maximum Expected Value (MEV) mass of COM, kg	Impacts CCRS launched mass allocation
	OS Mass	Maximum Expected Value (MEV) mass of OS, kg	Impacts SRL, MAV, EEV, and CCRS mass allocations
System Complexity	Number of Actuators in COM	Number of devices that moves and controls a mechanism (motor + gearbox) in COM, #	Impacts mass, cost, and risk
	Number of Unique Elements in COM	Number of unique elements in COM that require a dedicated engineer, WBS line items, development program, and qualifications program, #	Impacts risk, development cost, qualification cost, workforce needs, and interface management
Spacecraft Resources	Peak Power	Peak power draw during orientation operation, W	Drives power draw requirements from spacecraft
Orientation Station Performance	OS Rotatability	Ability to orient the OS in all orientations, Yes/No	Enables visual inspection of all surfaces of the OS prior to containment

4. SYSTEM DESIGN

Two flux pinning architectures for the Capture and Orientation Module were developed: one based on the MACARONE architecture configuration [6] (see Fig. 5), which passes the OS between stations along an arc, and the other based on inline architecture configuration, which passes the OS through stations in a linear fashion (see Fig. 6). For the MACARONE configuration, flux pinning assemblies with two different OS magnet arrangement were studied: one with twelve magnets all aligned with their poles in a vertical orientation (icosahedron extended dipole magnet arrangement), and another with twelve magnets all aligned with their poles facing outward from the center of the OS (icosahedron isotropic magnet arrangement). For the inline configuration, a single flux pinning assembly with one OS magnet arrangement was studied: six magnets around the equator, all aligned with their poles in a vertical orientation (equatorial ring magnet arrangement). A Thales LPT6510 pulse tube cooler is assumed for the cryocooler for superconductor field cooling.

Flux Pinning Configurations

The three flux pinning configurations for the OS, (icosahedron extended dipole, icosahedron isotropic, and equatorial ring magnet arranges) are described below. For each description, diagrams of the magnet arrangement on

the OS, the superconductor and cryocooler arrangement on flux pinning assembly that makes up the COM Orientation Station, the overall COM architecture configuration, and the general COM concept of operations are provided.

Icosahedron Extended Dipole Arrangement—In the icosahedron extended dipole arrangement, magnets would be placed on twelve locations equally spaced around the OS in the form of an icosahedron. All twelve magnets would be aligned with their poles parallel to the OS reference axis (see Fig. 11). The flux pinning assembly would consist of three superconductors, angled 116° from one another to align with the icosahedron magnet geometry on the OS (see Fig. 12). A cryocooler mounted to the assembly would cool the three superconductors for training and operation. The superconductors would be trained to flux pin the OS in an upright configuration, as shown in Fig. 13. The icosahedron extended dipole flux pinning assembly mounted in the Orientation Station of the Capture and Orient Module for a MACARONE architecture configuration is shown in Fig. 14. A concept of operations for a Capture and Orient Module using the icosahedron extended dipole flux pinning arrangement for OS orientation is shown in Figs. 15 and 16.

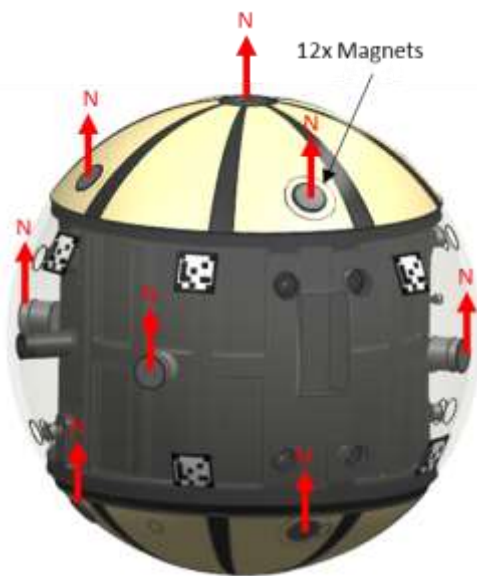


Figure 11. Icosahedron extended dipole magnet arrangement.

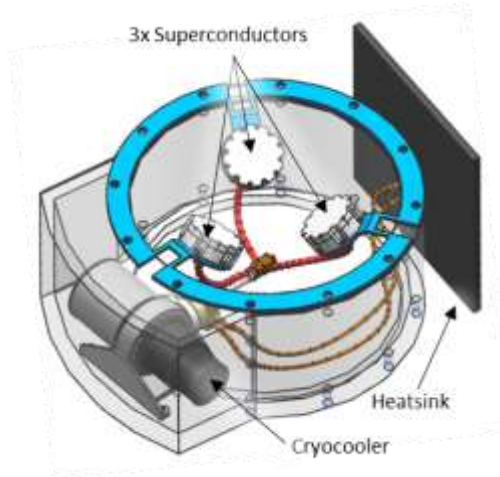


Figure 12. Icosahedron extended dipole flux pinning assembly.

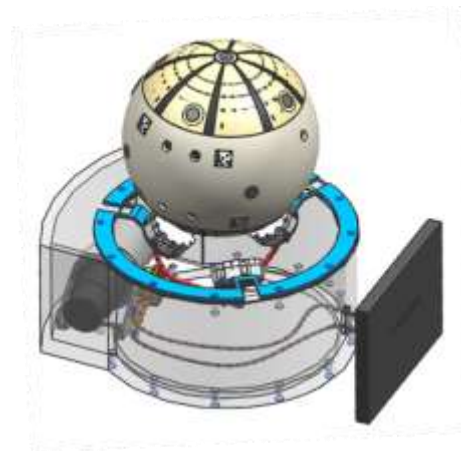


Figure 13. Icosahedron extended dipole flux pinned OS configuration.

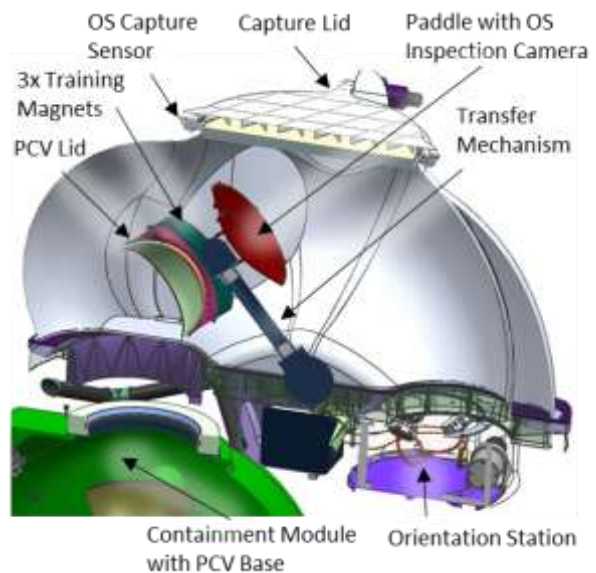


Figure 14. MACARONE icosahedron extended dipole Capture and Orient Module configuration.

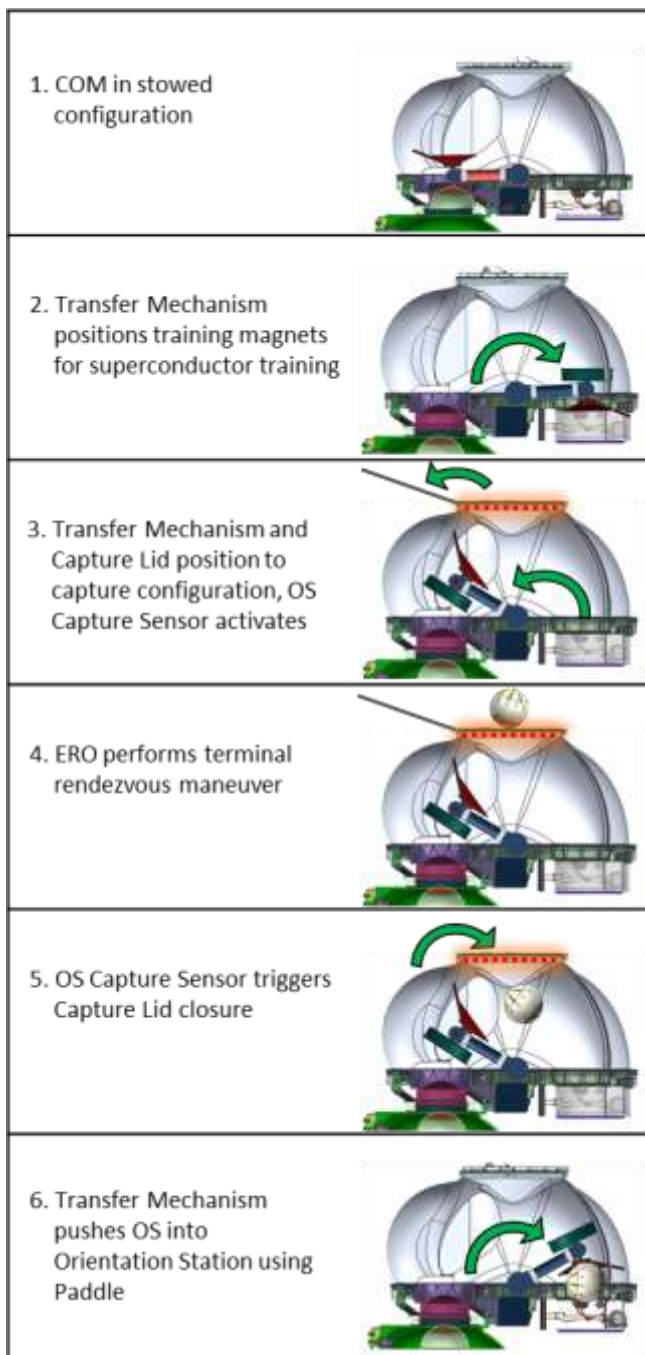


Figure 15. Icosahedron extended dipole Capture and Orient Module concept of operations, Part 1.

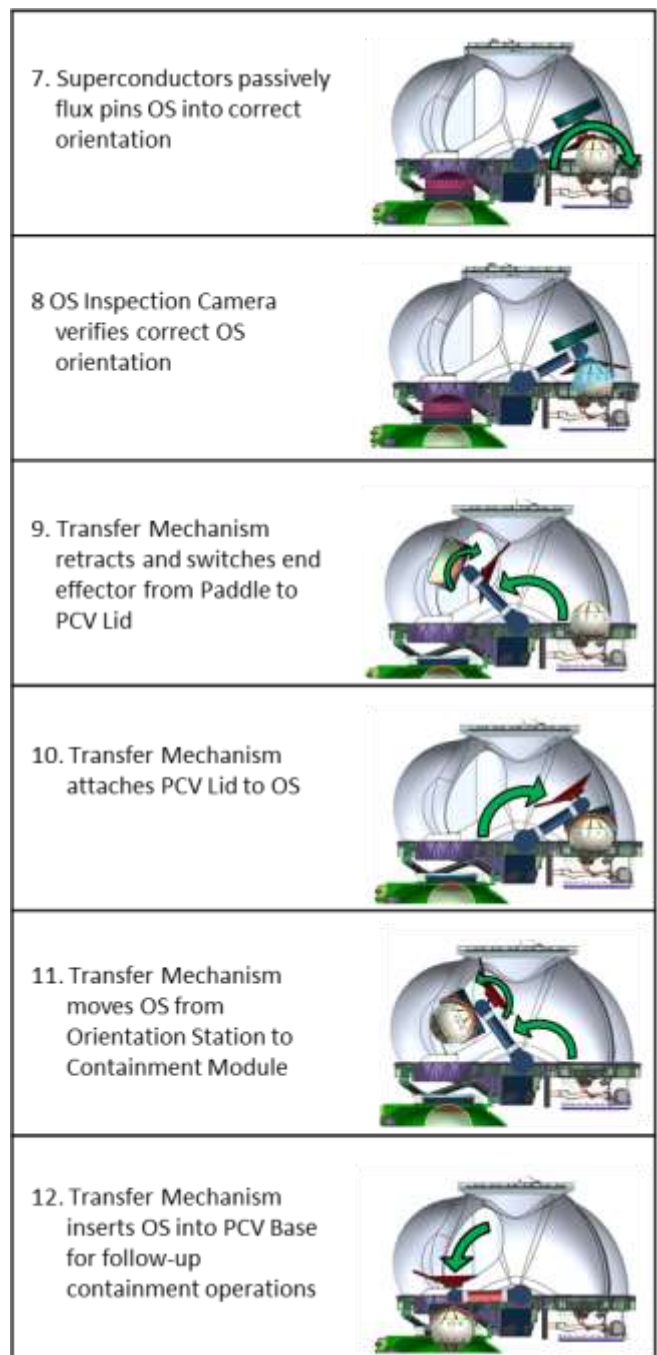


Figure 16. Icosahedron extended dipole Capture and Orient Module concept of operations, Part 2.

Icosahedron Isotropic Arrangement—In the icosahedron isotropic arrangement, magnets would be placed on twelve locations equally spaced around the OS in the form of an icosahedron. All twelve magnets would be aligned with their poles pointing away from the OS center (see Fig. 17). The flux pinning assembly would consist of three superconductors, angled 116° from one another to align with the icosahedron magnet geometry on the OS, as well as six electromagnets for rotating the OS (see Fig. 18). A cryocooler mounted to the assembly would cool the three superconductors for training and operation. The three superconductors would be trained to flux pin the OS with

any triangular magnets pattern on the OS, holding the OS in one of 36 unique stable poses. The electromagnetics would then activate, deforming the magnetic fields of the magnets to rotate the OS through new sets of stable poses until the OS ends up in the preferred orientation, as shown in Fig. 19. The icosahedron isotropic flux pinning assembly mounted in the Orientation Station of the Capture and Orient Module for a MACARONE architecture configuration is shown in Fig. 20. A concept of operations for a Capture and Orient Module using the icosahedron isotropic flux pinning arrangement for OS orientation would follow a similar set of operations as the icosahedron extended dipole flux pinning arrangement, with the exception added operations in Step 7 for electromagnetic orientation, as shown in Fig. 21.

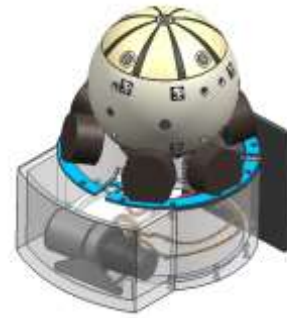


Figure 19. Icosahedron isotropic flux pinned OS configuration.



Figure 17. Icosahedron isotropic magnet arrangement.

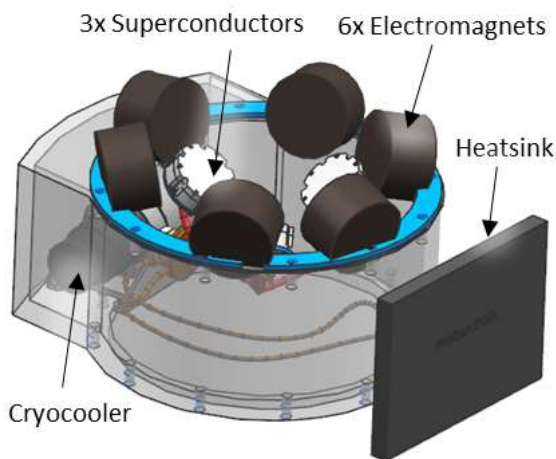


Figure 18. Icosahedron isotropic flux pinning assembly.

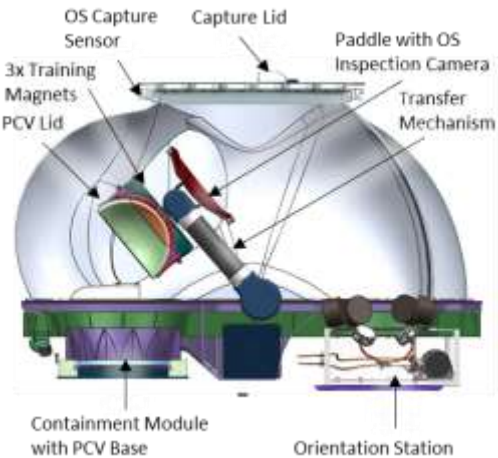


Figure 20. MACARONE icosahedron isotropic Capture and Orient Module configuration.

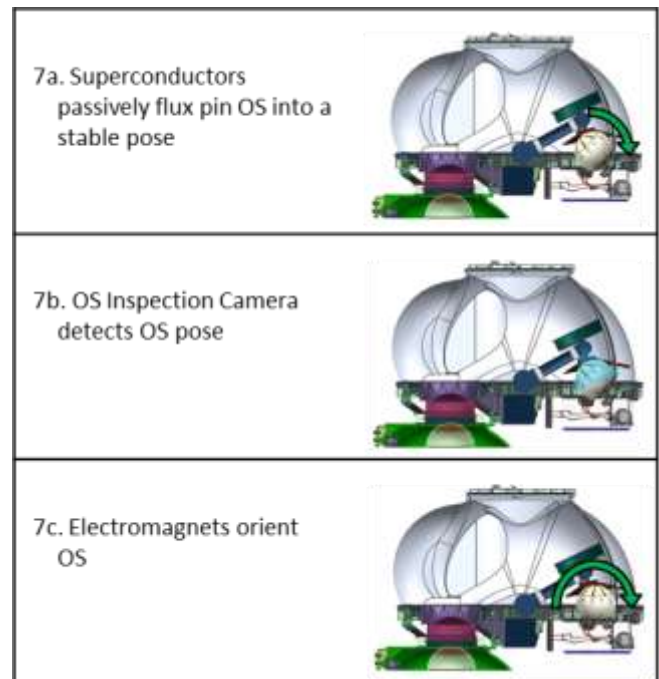


Figure 21. Icosahedron isotropic Capture and Orient Module concept of operations (Steps 1-6 and 8-12 are the same as the Icosahedron extended dipole Capture and Orient Module concept of operations in Figs. 15 and 16).

Equatorial Ring Arrangement—In the equatorial ring arrangement, magnets would be placed on six locations equally spaced around the equator of the OS. All six magnets would be aligned with their poles parallel to the OS reference axis (see Fig. 22). The flux pinning assembly would consist of three superconductors, equally spaced 120° around the perimeter and facing towards the central axis (see Fig. 23). A cryocooler mounted to the assembly would cool the three superconductors for training and operation. The superconductors would be trained to flux pin the OS in an upright configuration, as shown in Fig. 24. The inner diameter of the flux pinning assembly would be large enough to allow assembly of the PCV Lid onto the OS, as well as passages of the assembled PCV Lid and OS to allow final assembly to the PCV Base in the Containment Module. The equatorial ring assembly mounted in the Orientation Station of the Capture and Orient Module for an Inline architecture configuration is shown in Fig. 25. A concept of operations for a Capture and Orient Module using the equatorial ring flux pinning arrangement for OS orientation is shown in Figs. 26 and 27.

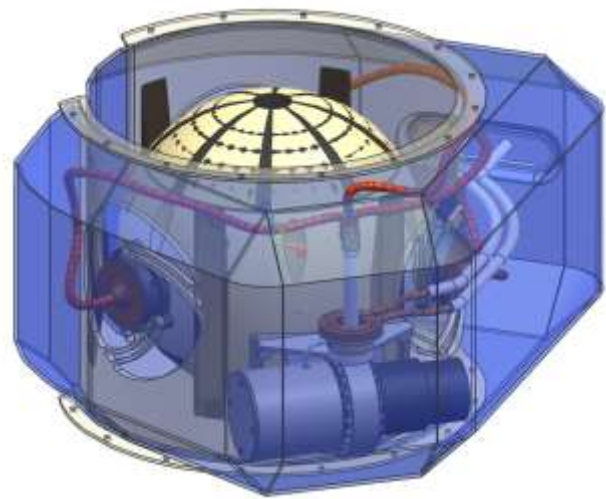


Figure 24. Equatorial ring flux pinned OS configuration.



Figure 22. Equatorial ring magnet arrangement.

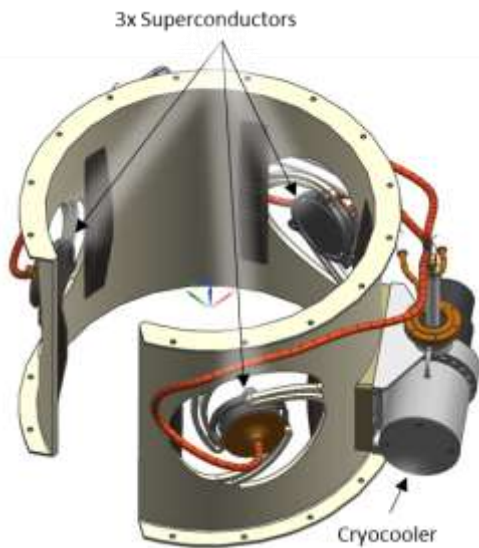


Figure 23. Equatorial ring flux pinning assembly.

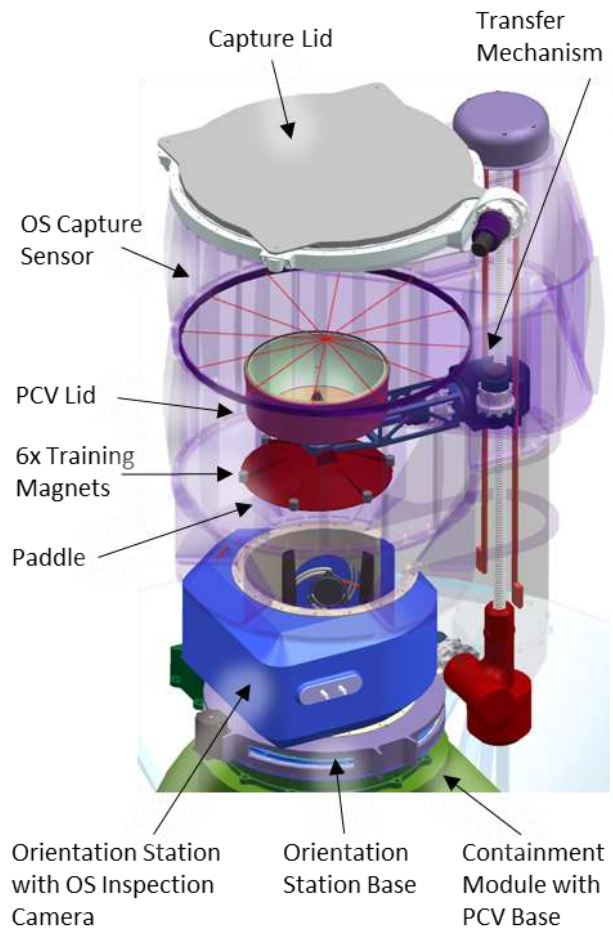


Figure 25. Inline equatorial ring Capture and Orient Module configuration.

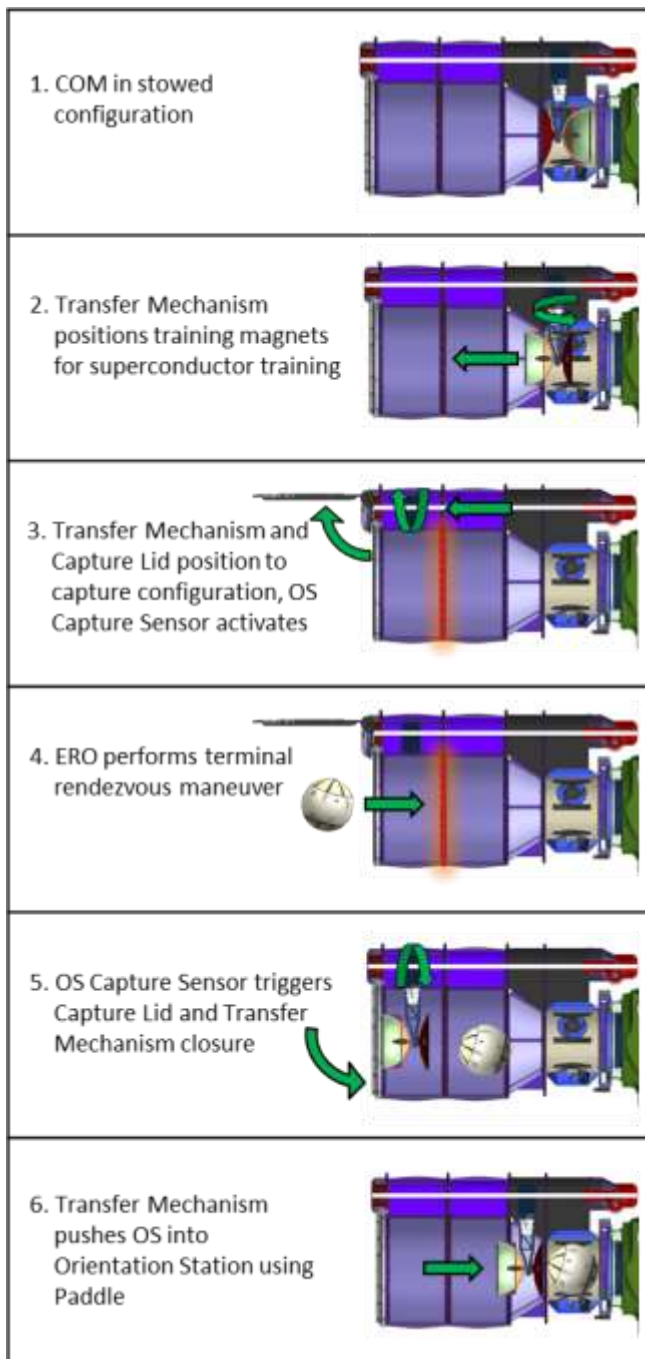


Figure 26. Equatorial ring Capture and Orient Module concept of operations, Part 1.

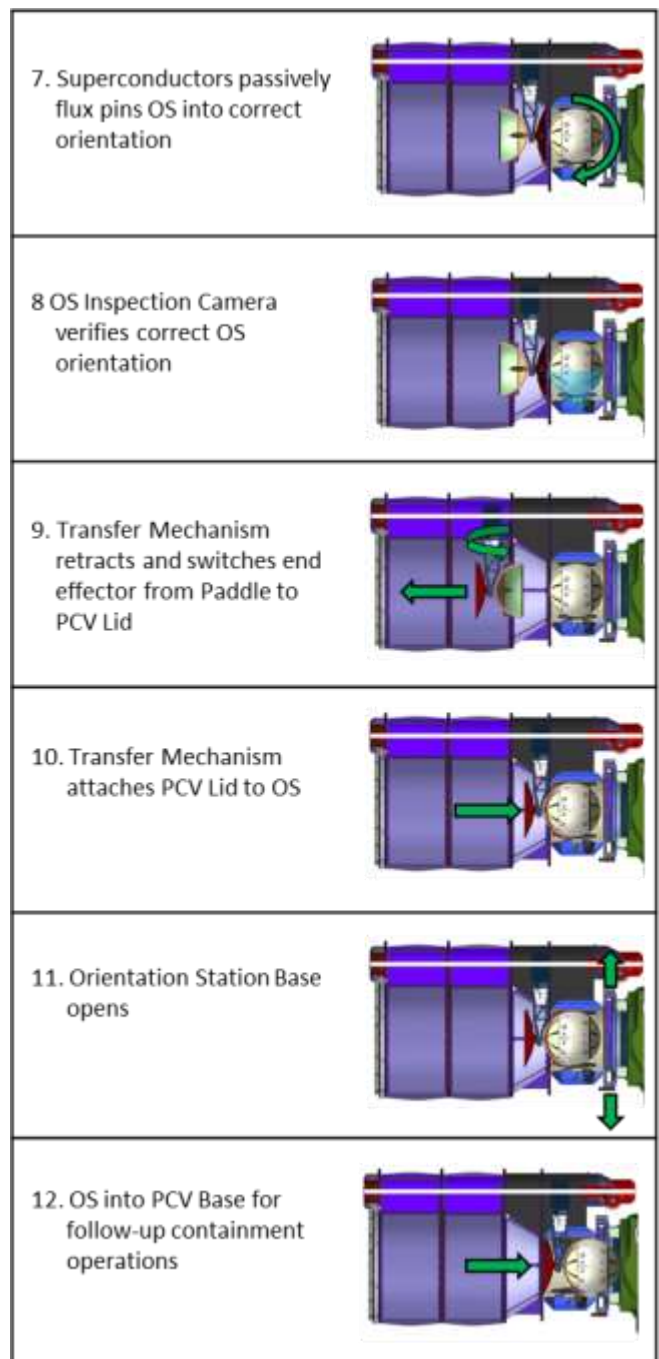


Figure 27. Equatorial ring Capture and Orient Module concept of operations, Part 2.

Alternate Flux Pinning Configurations—Alternate configurations were also looked at for cases where the OS comes in sterile (there are no significant amounts of unsterilized Mars particles on the outside the OS at the time of OS capture), and cases where the OS is non-spherical (a pill-shaped O would lower the mass of the containment vessels and EEV).

When the OS is assumed to be sterile, the Capture and Orient Module does not need to worry about any unsterilized Mars particles liberating themselves from the OS and contaminating the spacecraft, and, therefore, does

not need to enclose the OS before contact. For the MACARONE flux pinning architectures, the MACARONE Shell and Capture Lid could potentially be removed (see Fig. 28), lowering the system mass. However, the flux pinning assembly and magnets on the OS may need to be larger and stronger to perform OS capture in addition to OS orientation. For the Inline flux pinning architecture, the Capture Lid could potentially be removed (see Fig. 29), also lowering the system mass. Since the Transfer Mechanism would still participate in OS capture, no new functionality would be required of the flux pinning assembly.

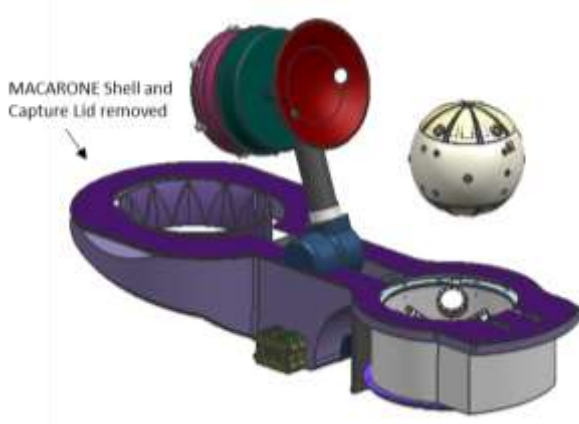


Figure 28. MACARONE Capture and Orient Module alternative configuration for a sterile OS.

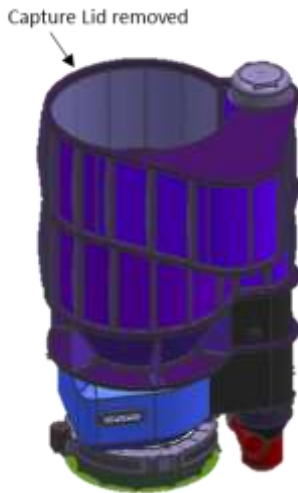


Figure 29. Inline Capture and Orient Module configuration for a sterile OS.

Flux pinning can be accomplished with a non-spherical OS for both icosahedron and equatorial ring magnet arrangements (Figs. 30-31). To have the same OS reorientation performance as the spherical OS configurations, stronger magnets may be necessary, and some of the magnets may need to move closer to the center of the OS due to the decrease in the OS outer diameter. This would increase the magnetic field that would need to be shielded against, leading to an increase in shielding mass. More analysis would need to be run on these OS

configurations to assess their performance and impact on OS mass.

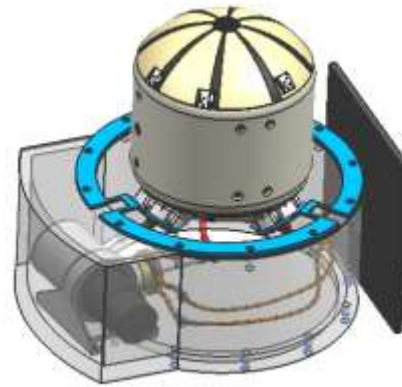


Figure 30. Icosahedron extended dipole flux pinned non-spherical OS configuration.

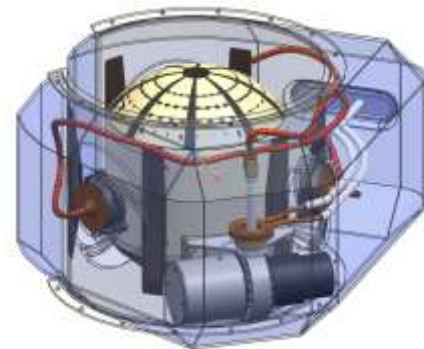


Figure 31. Equatorial ring flux pinned non-spherical OS configuration.

Cryocooler Design

A cryocooler would be required to bring the superconductors' temperatures below their critical temperature for the field cooling process. The cryocooler design is based off a Thales LPT6510 pulse tube cooler, shown in Fig. 32 [23]. The cooler is estimated to weigh 3.3 kg, has a maximum input power of 55 W, and includes mechanical mounting features and heat rejection surfaces. A 70 K temperature is anticipated for the flux pinning application.



Figure 32. Thales LPT6510 cryocooler.

5. ANALYSIS

Flux pinning and magnetic models were developed to provide tools to characterize and simulate the flux pinning process for system design, verification, and validation.

Flux Pinning Analysis

Flux pinning can be modelled a number of ways, but the basis for most analytical models is Kordyuk's Frozen Image Model [24]. The Frozen Image Model assumes infinite superconductor surfaces and perfect dipoles and creates a set of "images" of the magnets in the system, reflected over the surface of the superconductor, to approximate the attraction and repulsion forces experienced by a magnet in a field-cooled system. When derived for spacecraft [25], it is possible to use Villani's equations for the force and torque that a dipole exerts on another to derive the basic nonlinear equations of motion in a flux pinned system. Many model improvements have been developed to improve this approximation [26], [27], and these improvements represent the best analytical approach to capturing the dynamics of a complex multi-magnet, multi-superconductor system. Using this simplified modelling approach, it is possible to derive approximate forces and torques acting on a flux-pinned system and the predicted motion of the OS relative to the superconductor given a set of geometric and physical parameters and a set of initial conditions.

Fig. 33 shows the flux pinning model for an OS with an icosahedron isotropic magnet arrangement. Fig. 34 demonstrates the stability and rotational stiffness of the final orientation of the flux pinned OS through simulating a 5° offset about its x-axis.

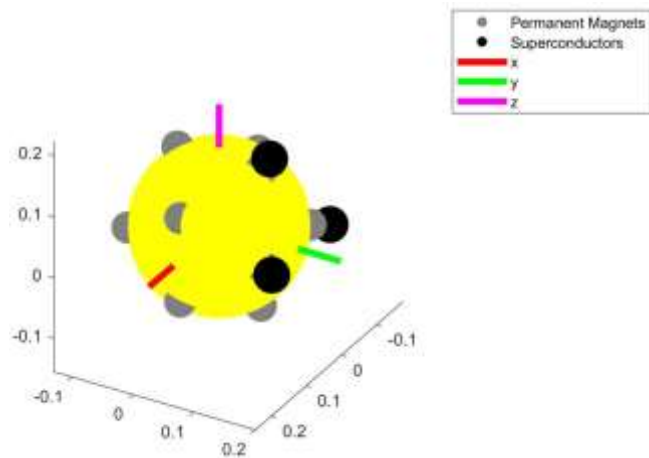


Figure 33. Icosahedron isotropic flux pinning model. All units are in meters.

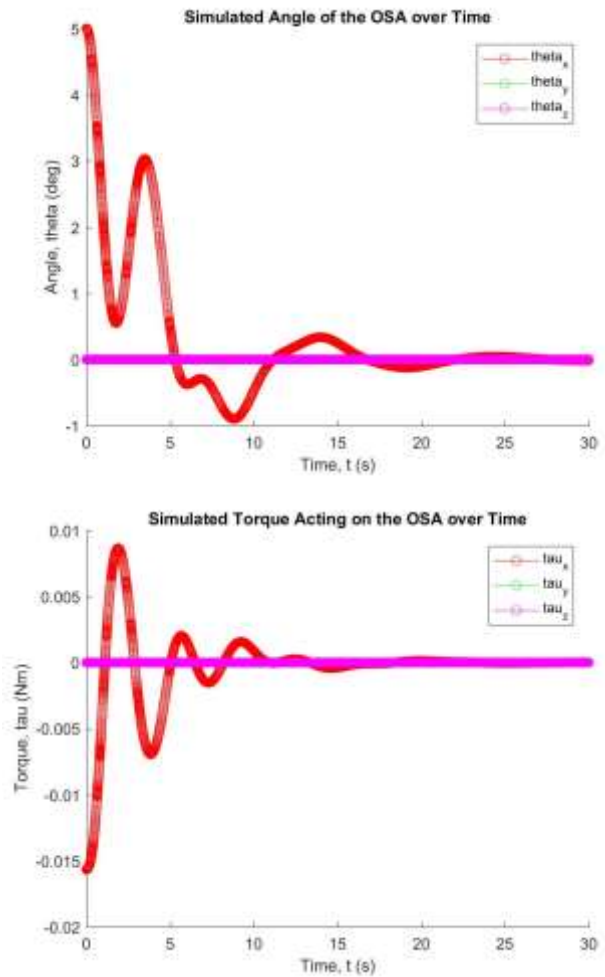


Figure 34. Simulated system response of a flux pinned OS with an equatorial ring magnet arrangement when submitted to a 5° offset about its x-axis.

Fig. 35 shows the flux pinning model for an OS with an equatorial ring magnet arrangement. Fig. 36 demonstrates the stability and rotational stiffness of the final orientation of the flux pinned OS through simulating a 5° offset about its x-axis.

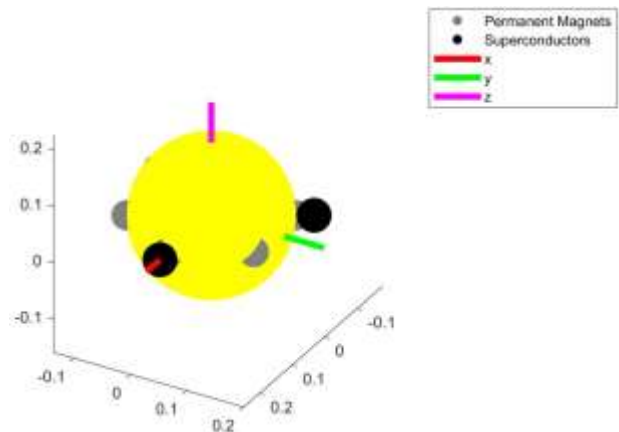


Figure 35. Equatorial ring flux pinning model. All units are in meters.

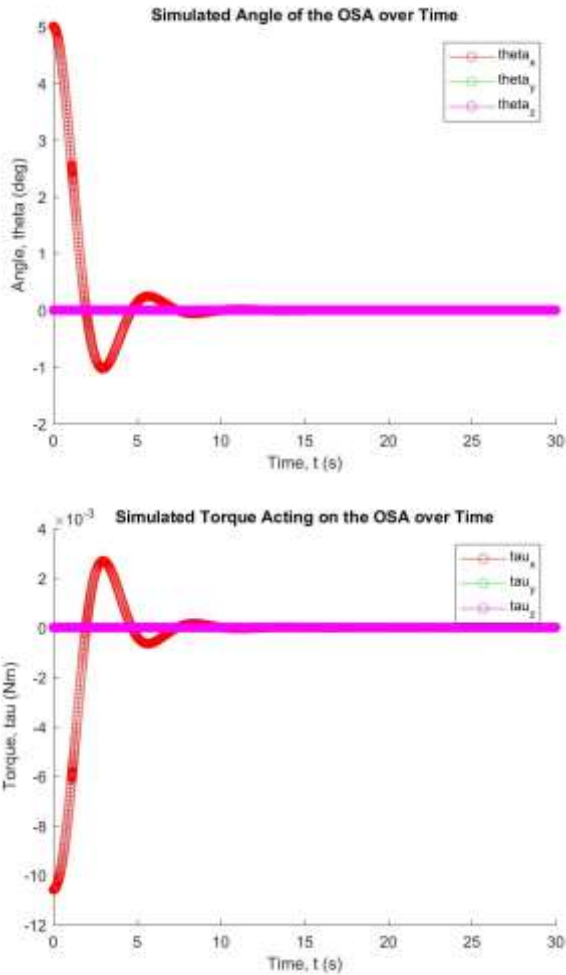


Figure 36. Simulated system response of a flux pinned OS with an equatorial ring magnet arrangement when submitted to a 5° offset about its x-axis.

OS Magnetic Shielding Analysis

A campaign-level science requirement to limit the Mars sample exposure to a 0.5 mT magnetic field was defined by the Returned Sample Science Board (RSSB), as documented by the International MSR Objectives and Samples Team (iMOST) [28]. To ensure this requirement is met while the sample tubes are in the OS, a 0.5 mT keep out zone was defined around the sample tubes, as shown in Fig. 37.

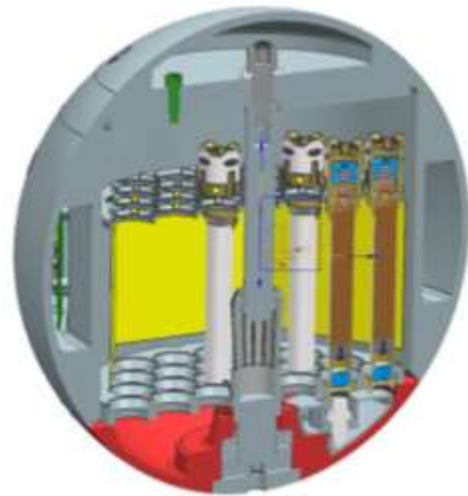


Figure 37. Keep out zone (shown in yellow) around the sample tubes 1 mm above and below the sample volume in the sample tubes.

Purpose—Magnetic modelling and simulation was performed to verify effectiveness of magnetic shielding to limit the sample exposure to a 0.5 mT magnetic field for the various flux pinning magnet arrangements, as well as estimate the added mass to the OS for the shielding.

Approach—Twelve spherical NdFe36 magnets were modelled within a 27 cm outer diameter zone within the OS for the icosahedron extended dipole and icosahedron isotropic magnetic arrangements, as shown in Fig. 38. Six cylindrical NdFe36 magnets were modelled within a 27 cm outer diameter zone within the OS for the equatorial ring magnetic arrangement, as shown in Fig. 39. A 0.43 mm thick, 0.775 kg AISI 1010 steel can was modelled around the sample tubes for magnetic shielding. Simulations were run for both tube insertion and assembled OS states.

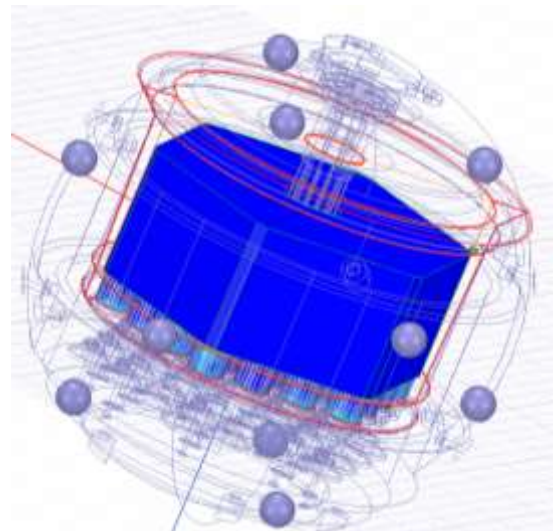


Figure 38. Magnet positions for the icosahedron extended dipole and icosahedron isotropic magnet arrangements.

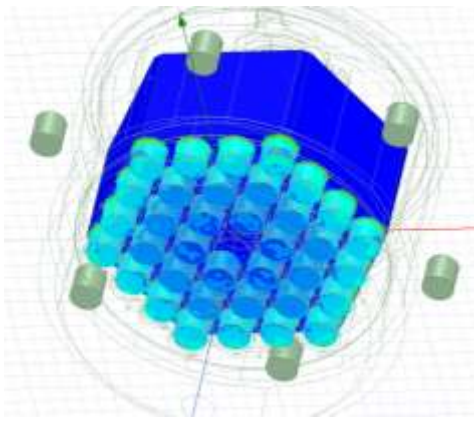


Figure 39. Magnet positions for the equatorial ring magnet arrangement.

Results—The simulation results for the OS icosahedron extended dipole, icosahedron isotropic, and equatorial ring magnetic arrangements are shown in Figs. 40-42. Magnetic fields of 0.5 mT or less are shown in dark blue.

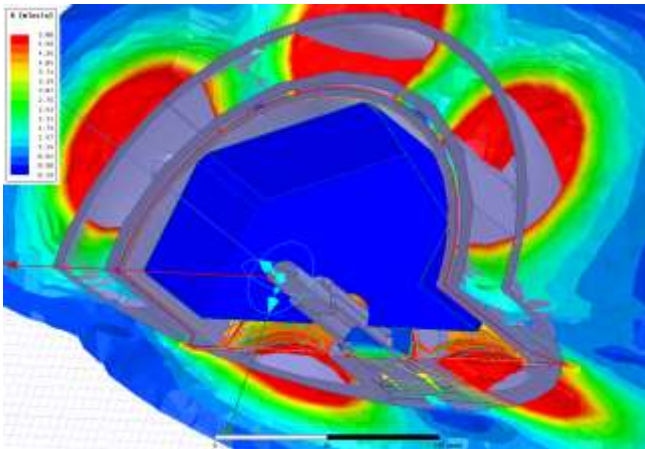


Figure 40. Shielding results for the icosahedron extended dipole magnet arrangement.

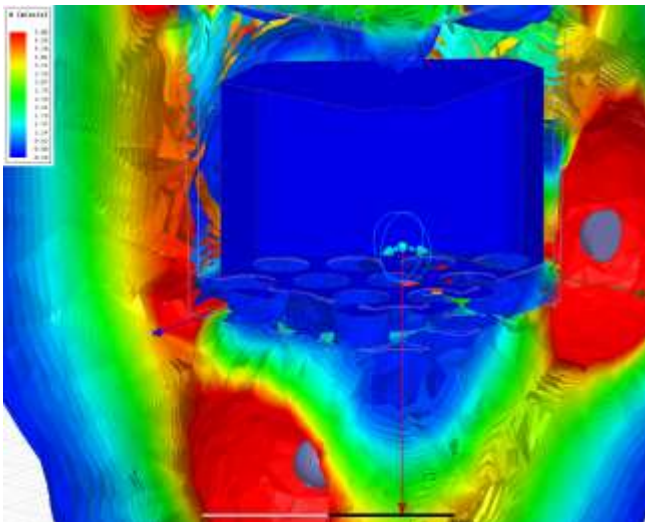


Figure 41. Shielding results for the icosahedron isotropic magnet arrangement.

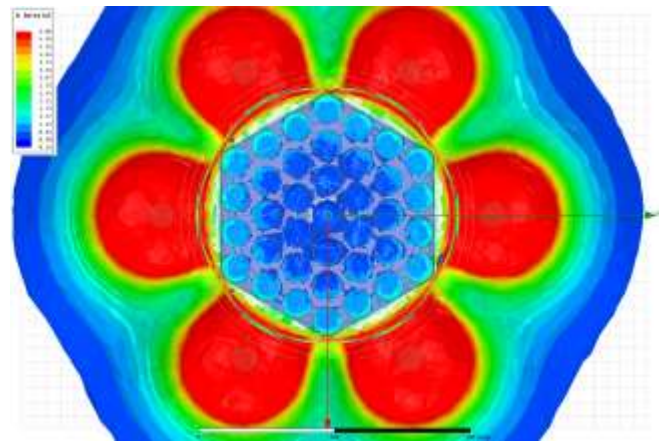


Figure 42. Shielding results for the equatorial ring magnet arrangement.

For the icosahedron extended dipole and icosahedron isotropic magnetic arrangements, the 0.43 mm thick, 0.775 kg shielding around the sample tubes was shown to meet the 0.5 mT requirement for all the samples. Assuming the main structure of the OS is aluminium, the potentially displaced mass of the aluminium would be 0.268 kg, leading to a net OS mass difference of 0.507 kg for shielding. For the equatorial ring arrangement, the 0.43 mm thick shielding was not sufficient to meet the 0.5 mT requirement for outermost samples. Therefore, thicker shielding would be required for this configuration.

6. EXPERIMENTAL TESTING

Tested was performed to demonstrate flux pinning for the icosahedron isotropic and equatorial ring magnet configurations, as well as collect flux pinning behavioral data for model development.

Microgravity Testing

A microgravity testbed, shown in Figs. 43-44, was developed to demonstrate OS capture in a microgravity environment. The testbed consisted of a Test Frame, a Sample Return Orbiter Analogue (SROA), an Orbiting Sample Analogue (OSA), and an OSA Launcher. The SROA contained a flux pinning device (see Fig. 45), comprised of a Thales LPT9310 cryocooler and three YBCO superconductors trained to pin an OS with an icosahedron magnet arrangement. Additional details about the design of the SROA flux pinning device are covered by McKinley et al. (2019) [17]. Additional details about the testing and results are covered by Zhu et al. (2018) [18].

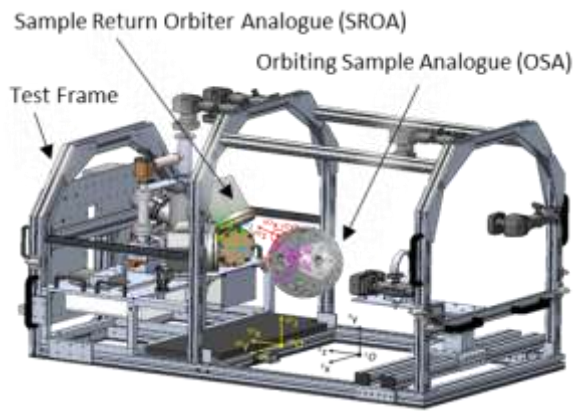


Figure 43. Microgravity testbed.

To track position and orientation of the OSA relative to the flux pinning device during microgravity testing, accelerometers were installed onto the Test Frame and inside the OSA. Additionally, a set of AprilTag fiducials were placed onto the OSA (see Fig. 46) and SROA flux pinning device (see Fig. 47) for visual tracking using a set of six cameras mounted around the Test Frame. Both 16H5 and 36H11 AprilTag families were used for the OSA and SROA. Positions and orientations of the AprilTag relative to the OSA and SROA reference frames were measured using a Zeiss COMET 3D scanner (Figs. 48-50). Visual estimation of the position and orientation the OSA relative to the SROA reference frame during test runs was calculated by tracking the AprilTags in the image sets using computer vision (Fig. 51). An example of the OSA tracking results using computer vision during a successful flux pinning capture test is shown in Fig. 52.

Sample Return Orbiter Analogue (SROA) Orbiting Sample Analogue (OSA) OSA Launcher



Figure 44. OSA Launcher delivering the OSA to the SROA during a microgravity test.

AprilTags on surface of OSA



Figure 46. AprilTag arrangement on OSA.

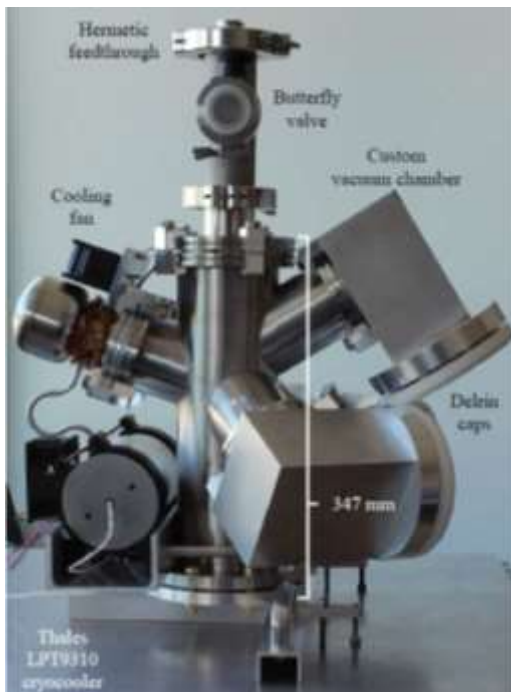


Figure 45. SROA flux pinning device. YBCO superconductor discs are mounted under each of the three Delrin caps [17].

AprilTags on faces of SROA



Figure 47. AprilTag arrangement on SROA flux pinning device.

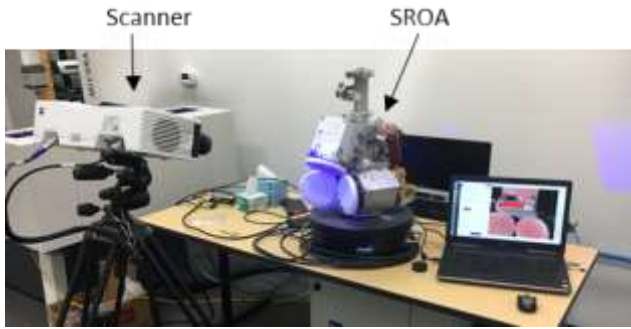


Figure 48. Zeiss COMET 3D scanner setup (Credit: Zeiss).

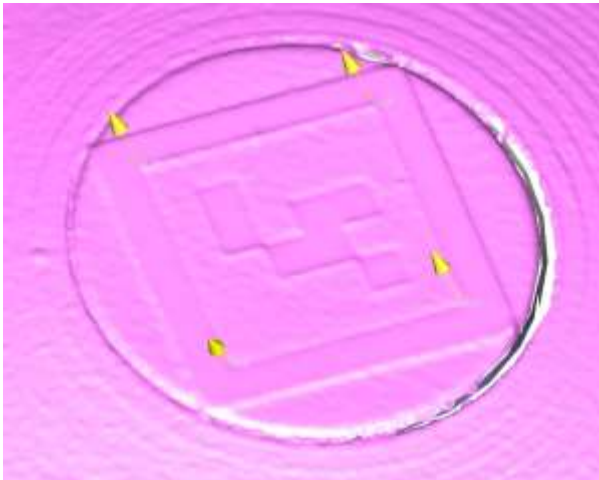


Figure 49. AprilTag corner locations were estimated based on visualization of the ink with the COMET scanner. Ink thickness was estimated to be ~10 microns, just at the limit of the instrument's resolution, but still visible due to the color and texture differences (Credit: Zeiss).

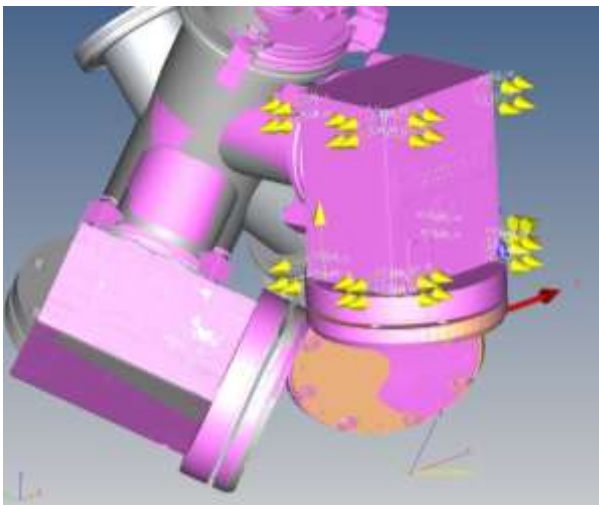


Figure 50. AprilTag position and orientation estimation relative to SROA reference frame (Credit: Zeiss).

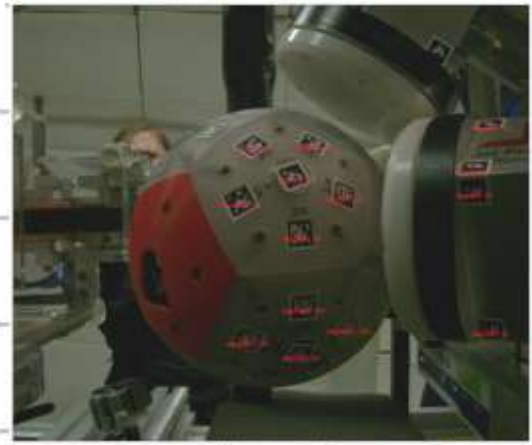


Figure 51. Detected AprilTags overlaid on an image taken of the flux pinned OS during microgravity testing.

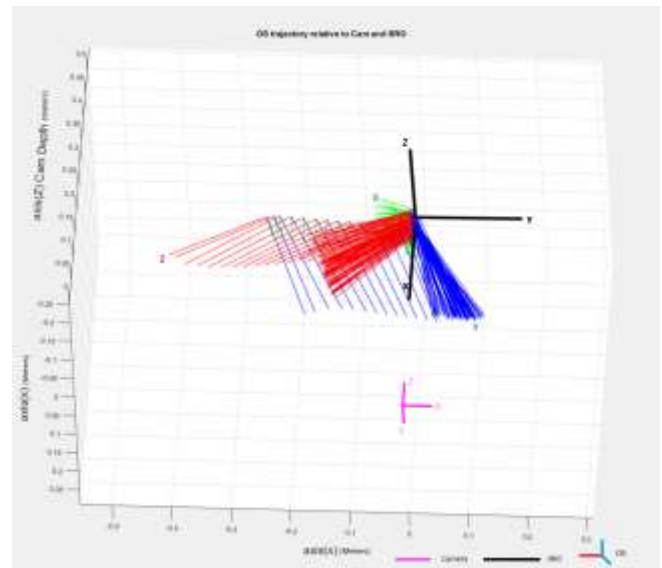


Figure 52. Plot of OSA position and orientation (the coordinate system shown in green/blue/red) relative to the SROA reference frame (the coordinate system shown in black) during a capture test based on AprilTag tracking. For reference, the coordinate system of the camera is shown in pink.

Orientation with Electromagnets Demonstration

OS orientation with flux pinning and electromagnets for an icosahedron isotropic magnet arrangement was demonstrated at Cornell University. The test setup for the demonstration is shown in Fig. 53. The OS contained 11 magnets arranged in an icosahedron isotropic arrangement. One of the twelve icosahedron vertexes was mounted onto a bearing to provide gravity offload for 1G testing. Testing demonstrated that the electromagnets were capable of rotating the OS.

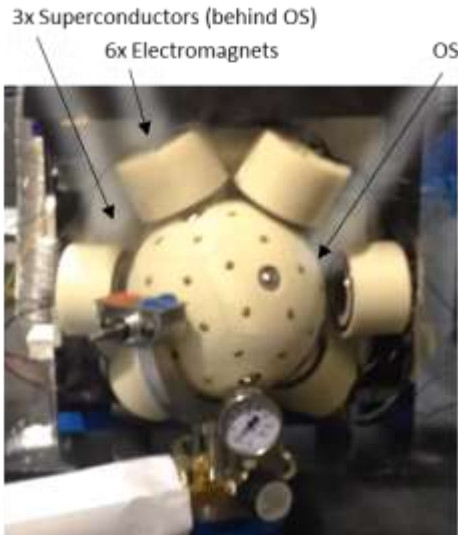


Figure 53. Test setup for OS orientation using flux pinning and electromagnets.

Equatorial Ring Arrangement Demonstration

Fluxing pinning with an equatorial ring magnet arrangement was demonstrated at JPL. The test setup for the demonstration is shown in Fig. 54. A half-scale, 14 cm diameter, 3D printed ring with thirty-six 5/16” diameter x 1/8” thick NdFeB, Grade N52 magnets was assembled to represent an equatorial ring magnet arrangement. Four 56 mm diameter x 16 mm thick YBCO superconductors were arranged around the ring, with a 1 cm radial gap between the ring and superconductors. A second ring of magnets was placed at the base of the fixture to provide gravity offload of the ring for 1G testing. Testing demonstrated that the ring of superconductors were capable of stably pinning the magnet ring in an upright orientation in the center of the testbed.

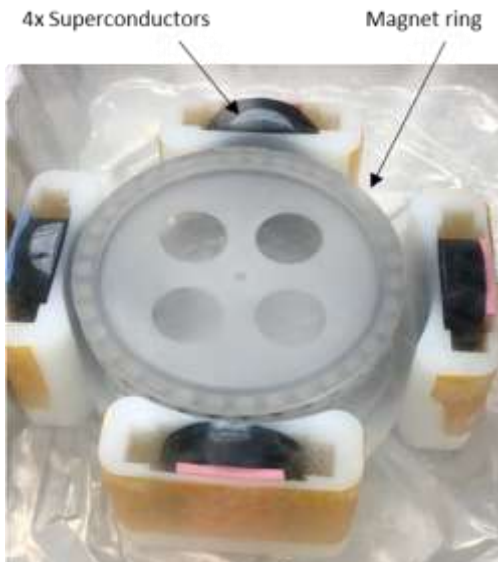


Figure 54. Flux pinning demonstration of an equatorial ring magnet arrangement.

5. DISCUSSION

A comparison of the three flux pinning Capture and Orient Module alternative configurations is shown in Tab. 2. Additionally, two non-flux pinning versions of the MACARONE and Inline architectures that use the Rotating Cups mechanism for orientation, described in more detail by Younse et al. (2018) [2], are listed on the rightmost two columns for further comparison. The flux pinning concepts would reduce the number of actuators required by the COM relative to the mechanical rotating cups equivalents, though would add mass to the COM and OS (due to the magnets and magnetic shielding), as well as draw more power. Only the MACARONE icosahedron isotropic arrangement of the flux pinning options would have the capability to rotate the OS. However, this would also draw a higher power due to the use of electromagnetics in parallel to the cryocooler during the OS orientation operation. Mass savings could be achieved if the OS was assumed to be sterile at time of capture, or if the OS was non-spherical (e.g., pill-shaped). Further analysis would be needed to quantify the mass savings for these configurations.

Table 2: Comparison of the flux pinning Capture and Orient Module alternative configurations.

Criteria		MACARONE Icosahedron Extended Dipole Flux Pinning	MACARONE Icosahedron Isotropic Flux Pinning	Inline Equatorial Ring Flux Pinning	MACARONE Rotating Cups	Inline Rotating Cups
System Mass	COM Mass	103 kg	116 kg	153 kg	101 kg	146 kg
	OS Mass	15.1 kg	15.1 kg	14.1 kg	12.0 kg	12.0 kg
System Complexity	Number of Actuators in COM	4	4	5	10	11
	Number of Unique Elements in COM	16	17	19	15	18
Spacecraft Resources	Peak Power	59 W	102 W	59 W	45 W	45 W
Orientation Station Performance	OS Rotatability	No	Yes	No	Yes	Yes

6. CONCLUSION

Flux pinning was shown to be a feasible technology for implementing on-orbit capture and orientation of a Mars Orbiting Sample container for potential Mars Sample Return. Benefits of the approach include passive, non-contact capture and orientation, as well as a reduction in the number of actuators relative to various mechanical methods. Flux pinning modeling showed the ability to model the flux pinning interactions for various magnet configurations, which could be used for further design studies, as well as

verification and validation of functionality. Magnetic modeling showed the ability to model the magnetic fields generated by the magnets around the OS and design effective shielding to ensure the sample exposure to the magnetic fields remain within acceptable limits. Prototype testing both in microgravity and 1G environments demonstrated feasibility for both OS capture and OS orientation using flux pinning in various magnet arrangements. A vision system using AprilTag fiducials tested on a free-floating OS in a micro-gravity environment demonstrated feasibility of using computer vision to estimate relative OS position and orientation.

ACKNOWLEDGEMENTS

The research described in this publication was carried out at the Jet Propulsion Laboratory of California Institute of Technology under contract from the National Aeronautics and Space Administration (NASA). The subject matter in this paper is pre-decisional, and for discussion purposes only.

REFERENCES

- [1] Committee on the Planetary Science Decadal Survey, Space Studies Board, "Vision and Voyages for Planetary Science in the Decade 2013-2022", *National Research Council of the National Academies*, Mar. 2012.
- [2] Younse, P., J. Strahle, M. Dolci, P. Ohta, K. Lalla, and E. Olds, "An Orbiting Sample Capture and Orientation Element Architecture for Potential Mars Sample Return," *2018 IEEE Aerospace Conference*, Big Sky, MT, Mar. 3-10, 2018.
- [3] Kornfeld, R., J. Parrish, S. Sell, and S. May, "Mars Sample Return: Testing the Last Meter of Rendezvous and Sample Capture," *Journal of Spacecraft and Rockets*, 44(3), Jun. 2007.
- [4] Mukherjee, R., B. Chamberlain-Simon, R. Smith, M. Dolci, R. McCormick, and P. Ohta, "Concepts for Mars On-Orbit Robotic Sample Capture and Transfer," *IEEE Aerospace Conference*, Big Sky, MT, Mar. 4-11, 2017.
- [5] Parrish, J., "To Mars and Back: Technologies for a Potential NASA Mars Sample Return," Mountain View, CA, Jun. 14, 2017.
- [6] Younse, P., R. Adajian, B. Cano, M. Dolci, P. Ohta, K. Lalla, V. Malyan, J. Munger, E. Olds, and J. Strahle, "Sample Capture and Orientation Technologies for Potential Mars Sample Return," *Proc. 2nd International Mars Sample Return 2018*, 6027, Apr. 25, 2018.
- [7] Davis, L., "Lateral restoring force on a magnet levitated above a superconductor," *Journal of Applied Physics*, vol. 67, no. 5, pp. 2631–2636, 1990.
- [8] Shoer, J. and M. Peck, "Flux-pinned interfaces for the assembly, manipulation, and reconfiguration of modular space systems," *Journal of Astronautical Sciences*, vol. 57, pp. 667–688, 2009.
- [9] Brandt, E., "Rigid levitation and suspension of high temperature superconductors by magnets," *American Journal of Physics*, vol. 58, no. 1, pp. 43–49, 1990.
- [10] Ma, K. B., Y. V. Postrekhin, and W. K. Chu, "Superconductor and magnet levitation devices," *Review of Scientific Instruments*, Vol. 74, No. 12, pp. 4989-5017, Dec. 2003.
- [11] Fujimoto, H., H. Kamijo, T. Higuchi, Y. Nakamura, and K. Nagashima, "Preliminary Study of a Superconducting Bulk Magnet for the Maglev Train," *IEEE Transactions on Applied Superconductivity*, Vol. 9, No. 2, pp. 301-304, 1999.
- [12] Shoer, J. P. and M. A. Peck, "Flux-Pinned Interfaces for the Assembly, Manipulation, and Reconfiguration of Modular Space Systems," *Journal of Astronautical Sciences*, vol. 57, no. 3, pp. 667–688, Jul. 2009.

- [13] Shoer, J. P. and M. Peck, "A Flux-Pinned Magnet-Superconductor Pair for Close-Proximity Station Keeping and Self-Assembly of Spacecraft," in AIAA Guidance, Navigation and Control Conference and Exhibit, Hilton Head, South Carolina, 2007.
- [14] Jones, L., W. Wilson, and M. Peck, "Design Parameters and Validation for a Non-Contacting Flux-Pinned Docking Interface," in AIAA SPACE 2010 Conference & Exposition, American Institute of Aeronautics and Astronautics, 2010.
- [15] Sorgenfrei, M. C., L. L. Jones, S. S. Joshi, and M. A. Peck, "Testbed Validation of Location-Scheduled Control of a Reconfigurable Flux-Pinned Spacecraft Formation," *Journal of Spacecraft and Rockets*, vol. 50, no. 6, pp. 1235–1247, 2013.
- [16] Zhu, F., L. Jones-Wilson, and M. Peck, "A Concept for Capturing and Docking Spacecraft with Flux-Pinned Interfaces," presented at the International Astronautical Congress, Guadalajara, Mexico, 2016.
- [17] McKinley, I., C. Hummel, and L. Jones-Wilson, "A Flight-Traceable Cryogenic Thermal System for Use in a Sample-Capture Flux-Pinned Interface," *IEEE Aerospace Conference*, Big Sky, MT, Mar. 2-9, 2019.
- [18] Zhu, F., M. Dominguez, L. Jones-Wilson, and M. Peck, "Flight-Experiment Validation of the Dynamic Capabilities of a Flux-Pinned Interface as a Docking Mechanism," *IEEE Aerospace Conference*, Big Sky, MT, Mar. 2-9, 2019.
- [19] Jones, L., W. Wilson, J. Gorsuch, J. Shoer, and M. Peck, "Flight Validation of a Multi-Degree-of-Freedom Flux-Pinning Spacecraft Model," in AIAA Guidance, Navigation, and Control Conference, Portland, Oregon, 2011.
- [21] Bar-Cohen, Y., M. Badescu, X. Bao, H. Jae Lee, S. Sherrit, D. Freeman, and S. Campos, "Synchronous Separation, Seaming, Sealing and Sterilization (S4) using Brazing for Sample Containerization and Planetary Protection," *Proc. SPIE 10168, Sensors and Smart Structures Technologies for Civil, Mechanical, and Aerospace Systems*, 101680A, Apr. 12, 2017.
- [22] Perino, S., D. Cooper, D. Rosing, L. Giersch, Z. Ousnamer, V. Jamnejad, C. Spurgers, M. Redmond, M. Lobbia, and T. Komarek, "The Evolution of an Orbiting Sample Container for Potential Mars Sample Return," *IEEE Aerospace Conference*, Big Sky, MT, Mar. 4-11, 2017.
- [23] Arts, R., J. Mullie, J. Tanchon, and T. Trollier, "LPT6510 Pulse Tube Cooler for 60-150 K Applications," *Cryocooler 19*, ICC Press, Boulder, CO, 2016.
- [24] Korodyuk, A., "Magnetic levitation for hard superconductors," *Journal of Applied Physics*, Vol. 83, No. 1, pp. 610-612, 1998.
- [25] Jones, L., "The Dynamics and Control of Flux-Pinned Space Systems: Theory and Experiment," Ph.D thesis, Cornell University, Ithaca, NY, 2012.
- [26] Zhu, F., M. Peck, and L. Jones-Wilson, "Reduced Embedded Magnetic Field in Type II Superconductor of Finite Dimension," Submiss.
- [27] Zhu, F. and M. Peck, "Linearized Dynamics of General Flux-Pinned Interfaces," *IEEE Transactions on Applied Superconductivity*, vol. 28, no. 8, pp. 1–10, Dec. 2018.
- [28] iMOST (co-chairs D. W. Beaty, M. M. Grady, H. Y. McSween, E. Sefton-Nash; documentarian B.L. Carrier; plus 66 co-authors), "The Potential Science and Engineering Value of Samples Delivered to Earth by Mars Sample Return," 186 p. white paper, posted August, 2018 by MEPAG at <https://mepag.jpl.nasa.gov/reports.cfm>, 2018.

BIOGRAPHY



Paulo Younse is a robotics engineer for the Robotic Vehicles and Manipulators Group at NASA's Jet Propulsion Laboratory in Pasadena, CA. His experience resides in mechanical design, machine vision, systems engineering, systems architecting, and planetary sample collection. He is currently working on the Mars 2020 rover developing the sample tube

hermetic seals to preserve samples for potential Earth return. Previous experience includes work on unmanned underwater vehicles at the Boeing Company and visual navigation and control for agricultural robots at the University of Florida. He received a B.S. in Mechanical Engineering from California Polytechnic State University, San Luis Obispo, and an M.E. in Agricultural Engineering from the University of Florida.



Laura Jones-Wilson earned her Bachelor of Science in aerospace engineering with a minor in mathematics in 2007. Laura graduated in the summer of 2012 with her Ph.D. in Aerospace Engineering, with a concentration in Dynamics and Controls and a minor in Astronomy.

She was awarded both the National Science Foundation (NSF) Graduate and the National Defense Science and Engineering Graduate (NDSEG) Fellowship. Presently, Dr. Jones-Wilson is a Guidance and Control Systems Engineer at NASA's Jet Propulsion Laboratory.



William Jones-Wilson is a Guidance and Control Hardware Engineer at NASA's Jet Propulsion Laboratory. He is currently working on the Mars 2020 Rover and the Europa Lander pre-project. Previous work experience includes mechanical and

aerospace engineering at Goodrich/Ithaco in Itasca, Ny. He earned his Bachelors degree in Engineering Sciences with a minor in astronomy in 2008 from Dartmouth College, and a Masters degree in Aerospace Engineering from Cornell University in 2009.



Ian McKinley received his B.A. and B.S. degrees, respectively, in physics and mechanical engineering from Occidental College and Columbia University in 2010 and a Ph.D. in mechanical engineering from UCLA in 2013. He is currently a thermal engineer in the Cryogenic Systems

Engineering group at NASA's Jet Propulsion Laboratory.



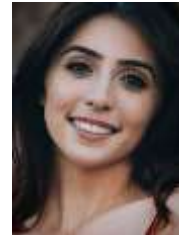
Chi Yeung Chiu is an undergraduate of Cal Poly Pomona, pursuing his degree in electromechanical engineering and hopes to continue his education in automation and robotics. Previously, he worked at NASA's Jet Propulsion Laboratory developing and testing designs for hermetic seal components for

the Mars Sample Return campaign. Currently, he is exploring end effectors for a robotic arm that can perform compliant assembly of a Primary Containment Vessel for Orbiting Sample Containment.



Eric Olds is a Mechanical Systems Engineer contracting to NASA's Jet Propulsion Laboratory from Sierra Lobo, Inc. He has over 20 years of experience working in engineering, and has worked extensively in electronics packaging, RF amplifier housings, mechanical structures, and mechanisms for space flight. He was the lead Mechanical

Engineer on the CheMin science instrument operating on the Mars Science Laboratory (Curiosity) Rover. Previous experience includes spacecraft operations and systems testing for Lockheed Martin. He received his B.S. in Aerospace Engineering from the University of California, Los Angeles.



Violet Malyan is a Mechanical Engineer contracting to NASA's Jet Propulsion Laboratory from Sierra Lobo, Inc. She received her B.S. in Mechanical Engineering from University of California, Irvine. She has experience working on electronics packaging, mechanical structures, and structural

analysis. She has previously worked on projects like REASON, M2020, and Sherlock at JPL.

